7-2009

Unconventionally high and low frequency eddy current methods for material surface characterizations

Norio Nakagawa
Iowa State University, nakagawa@iastate.edu

Chester C.H. Lo
Iowa State University, clo@iastate.edu

UNCONVENTIONALLY HIGH AND LOW FREQUENCY EDDY CURRENT METHODS FOR MATERIAL SURFACE CHARACTERIZATIONS

N. Nakagawa and C. C. H. Lo

Citation: AIP Conf. Proc. **1211**, 1471 (2010); doi: 10.1063/1.3362242

View online: http://dx.doi.org/10.1063/1.3362242

View Table of Contents: http://proceedings.aip.org/dbt/dbt.jsp?KEY=APCPCS&Volume=1211&Issue=1

Published by the American Institute of Physics.

UNCONVENTIONALLY HIGH AND LOW FREQUENCY EDDY CURRENT METHODS FOR MATERIAL SURFACE CHARACTERIZATIONS

N. Nakagawa and C. C. H. Lo

Center for Nondestructive Evaluation, Iowa State University, Ames, IA 50011

ABSTRACT. This paper reports on a type of multiple frequency eddy current NDE methodologies. A specific focus was placed on a multiple low frequency methodology that is suitable for case depth characterization of case-hardened steel samples. A nominally uniform excitation field approach has been developed, and demonstrated to work for discriminating the case depths ranging between 1 mm and 6 mm, while meeting additional requirements of one-sided access and a finite stand-off distance.

Keywords: Eddy Current, Low Frequencies, Case Hardened Steel
PACS: 81.70.Ex, 81.40.Rs , 81.65.-b, 07.07.Df

INTRODUCTION

Efforts have been made in the area of advanced eddy current (EC) measurement methodology and application developments, aiming not only to the traditional crack-like defect detection and characterization, but also to surface materials characterization. This line of work utilizes various forms of multiple frequency techniques, such as swept frequency EC, pulsed EC, and modulated excitation EC methods. For instance, the recent residual-stress characterization project has led us to the development of a swept high-frequency EC (SHFEC) measurement method and model-based inversion software that provide us with a near-surface conductivity profiling capability on low-conductivity materials [1], applicable also to other surface characterization problems such as coating characterization, machining anomaly detection [2], and high-temperature corrosion evolution and its monitoring. Many of these applications require operations at unconventionally high frequencies such as 10-100MHz.

In contrast, there are other applications requiring extremely low frequency EC operations. This paper focuses on a type of such low frequency applications, i.e. case depth determination in steel samples. Specifically, we work with inductively hardened steel rods of case depths ranging between 1 mm and 6 mm. A typical carbon steel material has a relative permeability of ~100 and a conductivity of ~6 MS/m. The standard skin depth calculation shows that, for such a material, one may need to operate in the range of 5-200 Hz, in order to be sensitive to the said range of case depths.

CP1211, *Review of Quantitative Nondestructive Evaluation Vol.29,*
edited by D. O. Thompson and D. E. Chimenti

FIGURE 1. Photographs of induction-hardened steel rods of 30 mm in diameter and 100 mm long, made of S45C containing 0.45 wt% C.

The conventional EC technique for case-depth characterization is based on the use of encircling coils, which is suitable to cylindrical rods of a finite length. (For other electromagnetic case-depth characterization approaches, see, for example, Ref. [3].) However, practical parts rarely have simple cylindrical shapes, and thus encircling coils are far less applicable than desirable. There are other practical needs as well, driven by process control of production lines that produce a large number of parts. Such practical needs lead to specific requirements that demand the measurement methodology to permit (a) one-sided access to accommodate practical part geometry, and (b) a finite stand-off distance (lift off) to avoid sensor wear. Notice that the requirements render encircling coils and surface-riding sensors inapplicable. To meet the requirements, we developed a nominally uniform field drive approach with a sensor system containing an excitation coil wound on a U-shaped ferrite core. In what follows, we introduce our methodology and demonstrate the required capabilities.

EXPERIMENTAL SETUP

Case-Hardened Steel Samples

We are provided with rod-shaped induction-hardened steel samples of 30 mm in diameter and 100 mm in length (Fig.1). They are made from a batch of S45C steel containing 0.45 wt% C. Actually, four nominally identical sets of the samples were made, each set consisting of one untreated rod and six case-hardened rods of case depths ranging between 1 mm and 6 mm. One set was subsequently characterized destructively to provide measured depths, as listed in Table 1.

TABLE 1. Nominal and measured case depths obtained by destructive characterization, where the effective case depth is defined as the depth where the Vickers hardness is 450, while the nominal Vickers hardness is 700 on the surface and 200 in the core.

Sample	"Un-treated"	"1mm"	"2mm"	"3mm"	"4mm"	"5mm"	"6mm"
Nominal case depth (mm)	-	1	2	3	4	5	6
Measured case depth (mm)	-	1.09	1.95	3.04	4.02	4.68	5.68

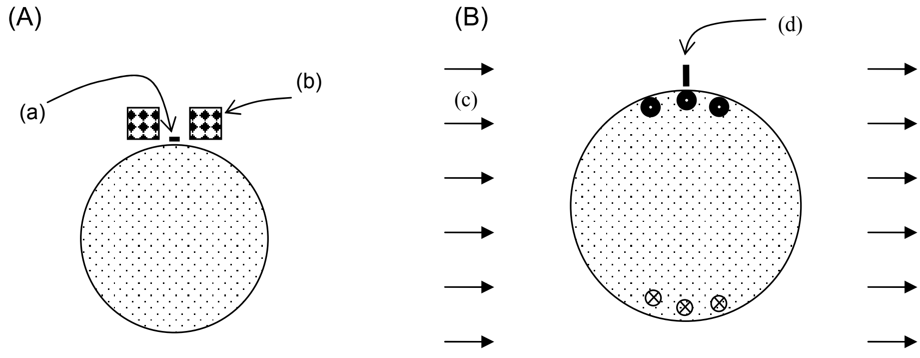

FIGURE 2. Schematic illustrations of possible one-sided access methods, (A) conventional and (B) proposed, both using a Hall device as a field detector [(a), (d)]. The two methods differ in the field excitation approaches, namely (A) by a side-mount coil [(b)] and (B) with a uniform incident field [(c)].

Nominally Uniform Field Drive and Detection Apparatus

As stated, our principal goal is to meet the requirement of one-sided access, which is traditionally approached by the side-mount coil excitation as illustrated in Fig. 2(A). However, this approach turns out to be unsatisfactory, basically because the sample geometry constrains the coil to be either small or curved to accommodate the part curvature. A small coil does not work well because it makes the detection too sensitive to the lift off, and because it further limits the field penetration depth by its size effect below the standard skin depth. Curved coils are impractical because they are bound to be component-specific in order to match the surface curvature. This work overcomes the difficulty by employing an alternative approach, namely the uniform field excitation method illustrated schematically in Fig. 2(B). When a component is immersed perpendicularly into a uniform incident AC magnetic field, eddy currents are induced on the top and bottom surfaces of the part, nearly uniformly along the surfaces. The nearly uniform "sheet" current generates locally uniform secondary fields that can be detected by the Hall device. The uniformity of the response field leads to one of the strengths of this methodology, i.e. increased robustness against the sensor lift off. The uniform field excitation also eliminates any size effects to the depth of penetration which, therefore, becomes equal to the standard skin depth.

Our detection apparatus to implement the uniform excitation field method is shown in Fig. 3. Nearly perfectly uniform field excitation would have been obtained by a field generator of a larger size than what is actually built, which is similar in size as the test sample. Nevertheless, our coil-core combination, consisting of a 281-turn coil of AWG 19 wire, wound around a U-shaped ferrite core, is found to generate sufficiently uniform magnetic field for our purpose in the space between the core yokes, when a steel sample is inserted. The sample space, i.e. the volume between the yokes, has approximate dimensions of 42 mm (height), 36 mm (gap), and 30 mm (length). At the bottom of the sample space, just above the coil, a Hall device IC chip is placed to face the bottom of the sample surface. The device detects the near-surface magnetic field at the sensitivity of 6.5 mV/gauss with the 5 V supply voltage. The IC package includes a built-in temperature compensation circuitry.

The electrical instrumentation consists of laboratory-grade instruments, i.e. a signal generator (Agilent 32250A) and a linear power amplifier (Kepco BOP-50-4) to drive the excitation coil, and a pre-amplifier (LeCroy DA1855A) and a DC power supply to detect the Hall device output while supplying the bias voltage. There are two output AC voltages

(A) (B)

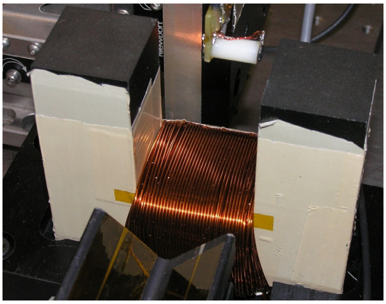

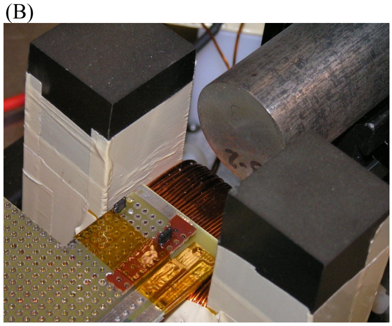

FIGURE 3. Photographs of the prototype uniform-field excitation-detection apparatus, showing (A) the exciter made of a drive coil wound around a ferrite core, and (B) the Hall device field detector. A nominally uniform field is generated in the space between the core yokes, when a steel sample is inserted, while the Hall sensor detects eddy current on the bottom surface of the sample.

to capture, one being the Hall device IC output V^o, and the other is the voltage V^{IR} across the current-sensing resistor R (R=1.33 Ω) inserted in series to the drive coil. The two voltages are digitized by a digitizer on a data acquisition board connected to a PC, triggered by the trigger signal out of the signal generator.

Time-Domain Mixed Multiple Frequency Operation

It is possible to operate the developed detector system in the ordinary constant frequency mode, with the signal generator generating a fixed frequency sinusoidal wave. However, for robust case depth characterization, multiple frequency data are indispensable. Instead of performing single frequency measurements multiple times, we here elected a faster time-domain operation where the drive voltage waveform is synthetically made of multiple frequency components, i.e.

$$V^D(t) = \sum_{k=1}^{N} V_k^D \sin k\omega_0 t \tag{1}$$

where ω_0 is the fundamental angular frequency (i.e. 2π times the repetition rate) and where a finite number of k-th harmonics V_k^D is selected to be non-vanishing. Technically, we digitally synthesize the waveform on the PC, download it to the function generator through GPIB, and let the function generator generate the corresponding analog waveform. The detected waveforms V^o and V^{IR} contain the corresponding frequency modes as

$$V^o(t) = \sum_{k=1}^{N} V_k^o \sin\left(k\omega_0 t - \alpha_k^o\right) \tag{2}$$

$$V^{IR}(t) = \sum_{k=1}^{N} V_k^{IR} \sin\left(k\omega_0 t - \alpha_k^{IR}\right) \tag{3}$$

from which respective Fourier components, both magnitudes and phases, can be extracted by Fourier transform to yield the transfer impedance for each frequency, calculated as

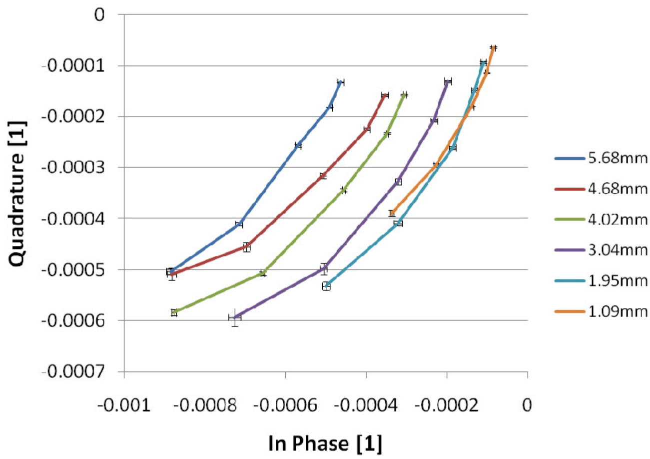

FIGURE 4. Impedance plane plots of the transfer impedances for the six case depth values (Table 1), nulled against the untreated sample signals. The curve for each thickness traces from small to large amplitudes as the frequency changes from 2 Hz to 32 Hz. Here, plotted are the averaged data with the error bars determined from nine sets of measurements, i.e. three rounds of measurements over the three sets of the samples, obtained with the 0.5 mm lift off.

$$Z_k = R \cdot \frac{V_k^o}{V_k^{IR}} e^{i\left(\alpha_k^o - \alpha_k^{IR}\right)} \tag{4}$$

The relative weights V_k^D of the drive voltage waveform are chosen so that the drive current waveform has nominally equal strengths V_k^{IR} among the selected frequency modes.

DATA-BASED CASE DEPTH DISCRIMINATION

We collected the transfer impedance data over the three sets of samples, by driving the nominally uniform field apparatus with the mixed multiple-frequency waveforms consisting of the harmonics of {1,2,4,8,16} with the repetition rate of 2 Hz. The transfer impedances were obtained according to the procedure, Eqs. (2~4), for each sample rod, including the untreated ones. For each sample set, we thus performed seven multiple frequency impedance measurements, and repeated the measurements over the three sets of the samples in three repetitions. For each of the nine sets of the measurement data, the signals were nulled against the untreated sample signals, namely, the signals from the untreated sample were subtracted from the case-hardened sample signals at each frequency. We then averaged the nulled data over the nine sets of measurements, with the corresponding estimates of the standard deviations. The resulting multiple frequency data are presented as the Lissajous plots in the impedance plane, as given in Figs. 4 and 5, with the frequency being the parameter. For each case depth, the locus traces from small to large amplitudes as the frequencies vary from 2 Hz to 32 Hz. The impedance data of Fig. 4 are taken with the stand-off distance (lift off) of 0.5 mm between the Hall device and the sample surface. The data acquisition method is robust against lift off as evidenced by the results for the lift offs of 0.25 mm and 1.0 mm, shown in Fig. 5. During the

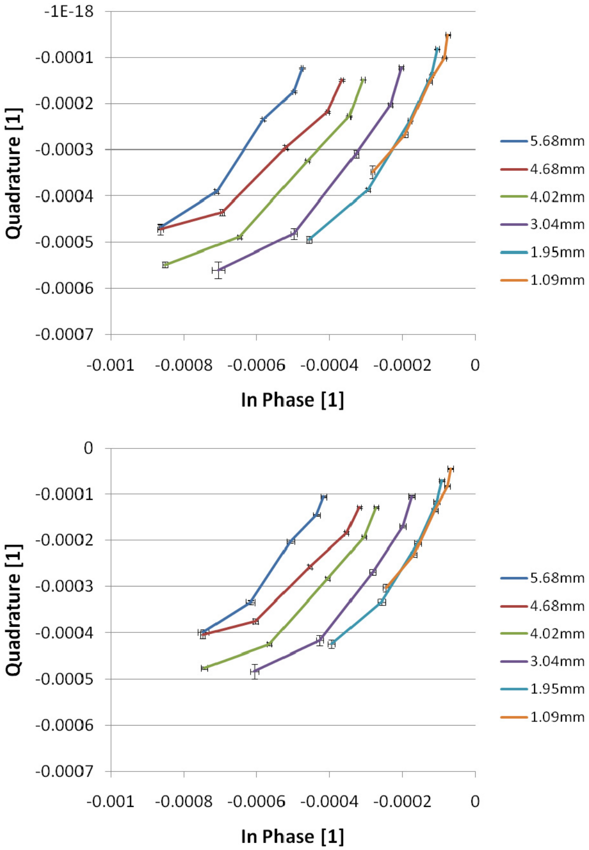

FIGURE 5. Transfer impedance plots similar to the one in Fig. 4, except that the upper result is obtained with the 0.25 mm lift off, while the lower result is for 1.0 mm lift off.

measurements, the lift off was controlled by the use of a plastic film of the appropriate thickness.

The result of Fig. 4 manifestly demonstrates the case depth discrimination capability for the depths of 3 mm to 6 mm, with clear separations outside the error bars, achieved at the 0.5 mm lift off. Moreover, the results of Fig. 5 demonstrate the robustness of the discrimination capability against the lift off in the range between 0.25 mm and 1.0 mm.

Although not manifest in the impedance plot, the same data given in Fig. 4 provide a robust procedure to separate the case depths between 1mm and 5 mm, when converted into phase data. To define relevant phase data, consider a pair of impedance data points of adjacent frequencies [e.g. $Z^{6mm}(8\ \mathrm{Hz})$ and $Z^{6mm}(16\ \mathrm{Hz})$] along each Lissajous curve [e.g. 6 mm], and calculate the impedance shift along the curve segment, for example,

$$\Delta Z^{6mm}(16-8\ \mathrm{Hz}) = Z^{6mm}(16\ \mathrm{Hz}) - Z^{6mm}(8\ \mathrm{Hz}). \tag{5}$$

In the plot of Fig. 4, such an impedance shift is represented geometrically by a vector connecting the pair of the adjacent frequency data points considered. Observe the

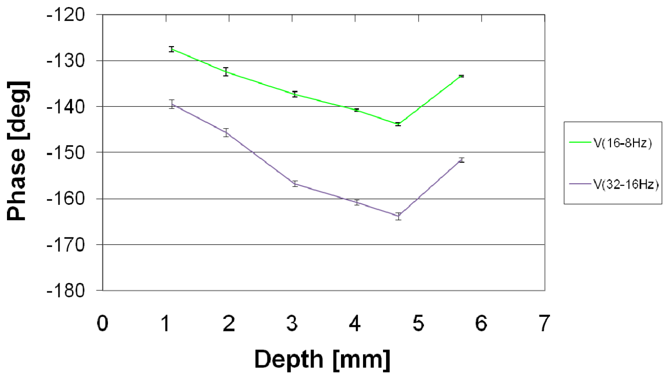

FIGURE 6. Plots of the phase vs. case depth correlation, where the "phase" data are calculated from the data of Fig. 4, as the phase of the impedance difference between adjacent frequencies.

behavior of such vectors in Fig. 4, and notice that the orientation of such vectors rotates systematically in the complex plane as the case depth changes from 1 mm to 6 mm. To exhibit this correlation quantitatively, we computed the impedance shifts defined by Eq. (5) between the adjacent frequency pairs, i.e. 8-16 Hz and 16-32 Hz, along all the Lissajous curves, and plotted the phases of the impedance shifts as functions of the case depth in Fig. 6. The result demonstrates that this type of the phase vs. case depth plots provides an unambiguous means to discriminate case depths in the range of 1 mm to 5 mm, based on the same data presented in Fig. 4.

It must be remarked that the underlying mechanism of the present case-depth discrimination method, and particularly the relevant material responses leading to the mechanism, is under investigation. Nevertheless, there exists a set of preliminary data which suggests strongly that nonlinear relations between the magnetic field and flux density, known to be present in steel materials, are playing an important role. Indeed, the data shows a significant disparity in the Rayleigh nonlinear parameters [4] between the case and core materials in our samples, presumably enabling our detection method.

CONCLUSIONS

This paper reports on a development of a multiple low-frequency EC method for case depth characterization in steels, based on nominally uniform-field drive approach. The detection system includes a nominally uniform EC inducer, consisting of an excitation coil wound around a U-shaped ferrite core. The resulting similarly uniform EC near the sample surface is detected by a Hall sensor. The output impedance signals have been shown to correlate with the case depths, thus providing a nondestructive method to discriminate case depths in steels in the range of 1 mm to 6 mm. Specifically, working with sets of case-hardened S45C steel samples, we obtained the data that demonstrated case-depth separation capabilities among 3~6 mm case depths in the complex impedance plane plots (Fig. 4), and among 1~5 mm case depths in the phase vs. case depth plots (Fig. 6). Unlike the conventional encircling coil method, this approach achieves the capability while meeting two additional requirements of one-sided access and a finite sensor lift off (0.5 mm or more).

ACKNOWLEDGMENTS

This work was supported by the NSF Industry/University Cooperative Research Program of the Center for Nondestructive Evaluation at Iowa State University. The authors thank T. Okuno of Toyota Motor Engineering & Manufacturing North America for providing the samples and their destructive characterization data.

REFERENCES

1. Y. Shen, A. M. Frishman, C. Lee, C.C.H. Lo, and N. Nakagawa, *J. Appl. Phys.* **101**, p. 014907 (2007).
2. C.C.H. Lo, and N. Nakagawa, "Detection of Anomalous Machining Damages in Inconel 718 and Ti 6-4 by Eddy Current Techniques," in *Review of Progress in QNDE,* this volume.
3. C.C.H. Lo, "Non-Contact Case Depth Measurements on Induction Hardened Steels by the Magnetic Hysteresis Method", 14th International Workshop on Electromagnetic Nondestructive Evaluation (ENDE), Dayton, Ohio, 2009.
4. R. M. Bozorth, *Ferromagnetism*, Van Nostrand, New York (1951), p. 476.